Structures 5 (2016) 186–195

Contents lists available at ScienceDirect

Structures

journal homepage: www.elsevier.com/locate/structures

Bond behavior of smooth and sand-coated shape memory alloy (SMA) rebar in concrete

A.H.M. Muntasir Billah, M. Shahria Alam *

School of Engineering, The University of British Columbia, Kelowna, BC, V1V1V7, Canada

ARTICLE INFO

Article history:
Received 18 June 2015
Received in revised form 16 November 2015
Accepted 25 November 2015
Available online 3 December 2015

Keywords:
Shape memory alloy
Rebar
Concrete
Compression bond strength
Slip
Pushout

ABSTRACT

The distinct superelastic properties and flag shape hysteresis of shape memory alloys (SMAs) make them an ideal candidate for the design and development of various structural components in civil infrastructure. Due to the fact that SMA reinforcement has significantly different properties than conventional steel, structures reinforced with SMA will behave differently. The design equations used for steel reinforced concrete structures are not applicable while using SMA as reinforcement in concrete. This study investigated the bond behavior of SMA rebars (with and without sand coating) in concrete using 56 pushout specimens. The test results are explored to evaluate the influence of concrete strength, bar diameter, embedment length, and surface condition. Surface modification using sand coating notably improved the bond strength of SMA rebar. Finally, empirical equation based on statistical analyses is presented to predict the maximum average bond strength. The proposed equation reasonably calculates the average bond strength of SMA reinforcing bars in concrete.

1. Introduction

Performance of reinforced concrete (RC) as a composite is significantly affected by the interaction of reinforcement and concrete which is referred as the bond strength. Bond strength–slip of rebar within concrete plays a critical role in the deformation of RC member [1]. Significant research has been conducted in this area to better understand the bond behavior of different types of rebars in concrete. Development length equations in the design of RC structures are established based on the bond strength. Different parameters affect the bond strength such as, bar geometries, concrete properties, presence of confinement around the bar, as well as surface conditions of the bar [2]. Over the past few years, researchers have experimented different applications of shape memory alloy (SMA) in civil infrastructure for improved performance of buildings and bridges during earthquakes [3–6]. However, little is known about the bond strength of SMA rebar with concrete. Since the surface condition and mechanical properties of SMA is completely different from regular steel rebar, it is imperative to investigate their bond properties before developing design equations and large scale industrial applications.

Conventional steel reinforcement possesses lugs or surface deformations which transfer the bond forces by mechanical interlock and friction. However, SMA rebars are usually produced in round shape with smooth surface without any deformation or lugs. Moreover, most of the commercially available SMA rebars are made of Ni–Ti alloy which is extremely hard and difficult to machine using conventional equipment [7]. On the other hand, threading of large diameter SMA rebars reduces the strength significantly [7]. Although the surface of SMA rebar is similar to the plain steel reinforcement found in historical structures, mechanical behavior of SMA bars, however, significantly differs from that of the plain steel reinforcing bars. Extensive experimental studies have been carried out by several researchers on the bond behavior of plain steel reinforcement [1,8–10]. However, no study has been undertaken so far to evaluate the bond behavior of SMA rebars with concrete. This justifies the need to conduct an experimental investigation of the bond behavior of SMA rebars embedded in concrete.

Several researchers have investigated and showed the efficacy of SMA as reinforcement in concrete structures [3–7]. However, for large scale application in construction industry, different structural aspects of SMA rebars should be investigated to ensure their reliable application. The interfacial bond behavior between SMA rebar and concrete is a governing factor in controlling the deformation of SMA–RC structures. Moreover, most of the applications of SMA rebar found in literature are focused on compression members such as columns and bridge piers. The compression bond behavior of reinforcement in concrete is significantly different for rebars in tension. Moreover, design codes suggest different development length equation for tension and compression development lengths. Very few studies [8,9] have reported the compression bond behavior of rebars embedded in concrete. This study is aimed at investigating the compressive bond behavior of SMA rebars embedded in concrete.

* Corresponding author. Tel.: +1 250 807 9397; fax: +1 250 807 9850.
E-mail addresses: muntasir.billah@alumni.ubc.ca (A.H.M. Muntasir Billah), shahria.alam@ubc.ca (M.S. Alam).

http://dx.doi.org/10.1016/j.istruc.2015.11.005
2352-0124/

SMA rebar is currently available with smooth surfaces. While using this smooth rebar as internal reinforcement in critical regions (e.g. plastic hinge region of a beam), a large major crack will be formed under loading. This crack will be flexural bond crack and the concrete section might experience shear failure at this location since no aggregate interlocking is available for resisting shear. Fig. 1 shows such condition, where SMA was used in the plastic hinge region of a beam-column joint and a large major crack was observed due to the use of smooth surfaced SMA rebar. However, for deformed or properly bonded bar, many small cracks will be formed and distributed over the whole plastic hinge length and can help resist more loading. In order to overcome the drawbacks of smooth SMA rebar, the surface of the smooth SMA bar was roughened using sand coating. Two different granulometries were used to evaluate the effect of surface roughness on the bond behavior of SMA rebar by means of providing improved interlocking in addition to mechanical adhesion. The objective of this experimental investigation is to study the compressive bond behavior of SMA rebar where the variables include SMA bar diameter, concrete strength, bonded length, concrete cover, and surface condition. Based on the experimental results, empirical equation for predicting the average maximum bond strength of SMA rebar has been developed. This research has practical significance since the outcome of the study will provide an understanding of the bond behavior of SMA rebar and will provide a basis for the development length prediction of SMA reinforced concrete members.

2. Research significance

Adequate bond strength between concrete and reinforcing bars has been identified as a cardinal parameter to the satisfactory performance of RC structures [2]. Over the past few years researchers have proposed and developed SMA reinforced concrete structures for improved seismic resistance. But no study has been undertaken to evaluate the bond behavior of SMA rebars with concrete. In order to increase the practical application of SMA rebars in concrete structures, it is required to identify the bond stress–slip behavior with concrete. Identification of the bond properties of SMA bars in concrete will allow for safe, reliable, and efficient use of SMA.

3. Experimental program

The experimental program conducted in this study involved a series of 56 pushout test specimens (concrete cylinders) with different parameters (Table 1). In this study, pushout test was selected since it was simple to conduct and to overcome the drawbacks associated with pullout test as described in Feldman and Bartlett [10].

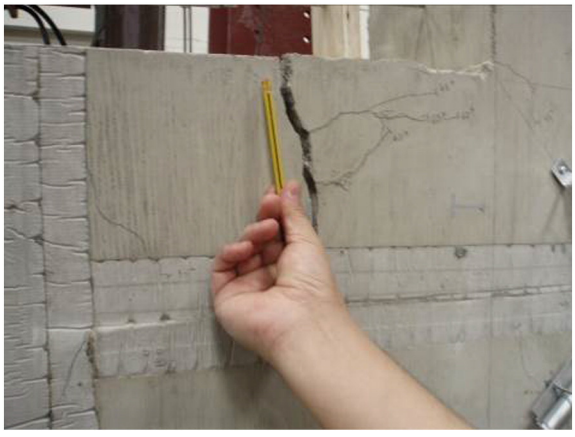

Fig. 1. Bond failure of concrete section having smooth SMA rebar. Adapted from [3].

Table 1
Pushout test specimens.

Bar size	Bar finish	l_d, mm	Concrete cover, mm	Compressive strength, MPa	Sample no., n
20 mm	Smooth	60	40	35	2
		100	40	35	2
		140	65	35	2
		180	65	35	2
		60	40	50	2
		100	40	50	2
		140	65	50	2
		180	65	50	2
		60	40	40	2
		60	40	60	2
	Sand-300	60	40	50	2
		100	40	50	2
		140	40	50	2
	Sand-600	60	40	50	2
		100	40	50	2
		140	40	50	2
32 mm	Smooth	96	34	35	2
		160	34	35	2
		224	59	35	2
		280	59	35	2
		96	34	50	2
		160	34	50	2
		224	59	50	2
		280	59	50	2
	Sand-300	96	34	50	2
		160	34	50	2
	Sand-600	96	34	50	2
		160	34	50	2
					Total = 56

3.1. Variables

A review of literature [8,9,11] on compressive bond behavior of reinforcement with concrete dictated that five different parameters need to be investigated to evaluate the bond behavior of SMA rebar with concrete [8–20]. The parameters include the following: concrete compressive strength (35, 40, 50, and 60 MPa; embedment length ($3d_b$, $5d_b$, $7d_b$, $9d_b$), bar diameter, d_b (20 mm and 32 mm), concrete cover (34 mm, 40 mm, 59 mm and 65 mm) and surface condition (smooth, sand coated). These parameters were selected based on materials availability, available testing facilities, and practical applications.

3.2. Materials

In this study, Ni–Ti SMA rebar (nitinol) has been used as reinforcement to investigate the bond behavior. The austenite finish temperature, A_f, which defines the transformation from martensite to austenite phase, ranges from −15 °C to −10 °C. All the Ni–Ti bars used in this study were 450 mm long. The yield strength of the SMA rebar was 401 MPa at a strain of 0.75% and the elastic modulus was 62.5 GPa, and the Poisson's ratio was 0.33. These values were provided by the SMA manufacturer.

Four different concrete mixes were considered for evaluating the effect of concrete compressive strength on the bond-behavior of SMA rebar. Similar type of cement, fine aggregate and coarse aggregate were used for different concrete mixes, while the proportions were varied accordingly to get the desired compressive strength.

3.3. Specimen preparation and testing

Cylindrical concrete specimens with dimensions of 100 mm × 200 mm and 150 mm × 300 mm (D × L) with SMA rebar at the center were used in this study. Fig. 2 shows the picture of few specimens after casting. The as-received bars were smooth and later the surface condition was modified using sand of two different granulometries. Two different sizes of sand, 300 μm and 600 μm were used to modify

Fig. 2. Specimens after casting.

the rebar surface and investigate the effect of surface modification on the bond behavior. G/Flex epoxy (west systems) was used as the adhesive to apply sand coating on the rebar. Using sandpaper, the rebars were cleaned to remove any dirt on the surface and the required embedment length was marked before applying the epoxy (Fig. 3a). A paint brush was used for applying the epoxy coating on the surface of each rebar (Fig. 3b), and subsequently, the epoxy coated rebars were rolled over the sand for sand coating (Fig. 3c). The total thickness of the epoxy and sand were between 1.5 mm–2 mm. Then the rebars were cured for 48 h for proper bonding (Fig. 3d). The embedment length of sand coated rebars are also shown in Fig. 3d.

For the pushout test, the concrete cylinder with the SMA bar at its center was placed on a metal frame with a circular plate at the top having a 35 mm hole at the center. Fig. 4 shows the test setup for the pushout test. The rebar was positioned in the cylinder in such a way that 50 mm of the rebar popped out beyond the top surface of the cylinder (loaded end), a certain length of the bar was embedded in concrete (i.e. the embedment length in Fig. 4), and the remaining portion protruded from the bottom of the cylinder (free end) to allow connection of the displacement sensors (string potentiometer). The embedment length was varied as shown in Table 1. In order to avoid stress concentration, a length of 25 mm at both the top and the bottom of the specimens was wrapped with plastics (i.e. the bond breaker in Fig. 4). A flat metal plate was placed on top of the SMA bar in order to apply the load evenly on the bar. The test was conducted in force control method using Instron testing machine and the projecting bar was pushed down by the actuator, and using a string potentiometer attached to the bottom of the protruding rebar, the slip of the rebar was measured at the free end. An electronic load cell equipped with the testing machine measured the load. Both the load and the rebar slip were recorded through the data acquisition system. The load was applied at a rate of 1–1.5 kN/s. The test was conducted until a slippage of 30 mm was recorded.

4. Experimental results

4.1. Failure modes

The pushout test specimens with smooth SMA bars failed at the concrete-rebar interface without developing any splitting crack. In smooth SMA rebar there was no surface deformation. Therefore, the bond force was transferred only by adhesion between the concrete and SMA rebar before any slip occurred. When the adhesion was lost, the bond mechanism developed due to the friction between the rebar and the small particles that broke free from the concrete upon slip, and the plain rebar simply slipped through the concrete. Fig. 5 shows the condition of the pushout specimens with plain rebar before and after testing. From Fig. 5a it can be seen that initially the rebar was protruded 50 mm from the top which finally got reduced to 20 mm at the end of the test (Fig. 5b) without any sign of splitting cracks. A closer look inside the cylinder (Fig. 5c) shows that there was no significant bond between the smooth SMA rebar and concrete as shown by the smooth surface of the concrete.

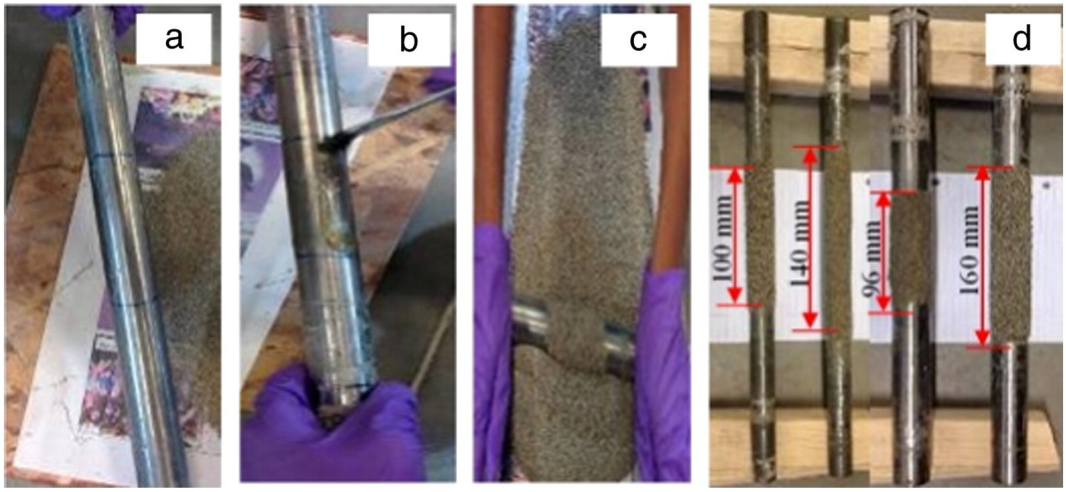

Fig. 3. Sand coating of SMA rebar (a) bonded length, (b) epoxy application, (c) sand coating and (d) sand coated rebars.

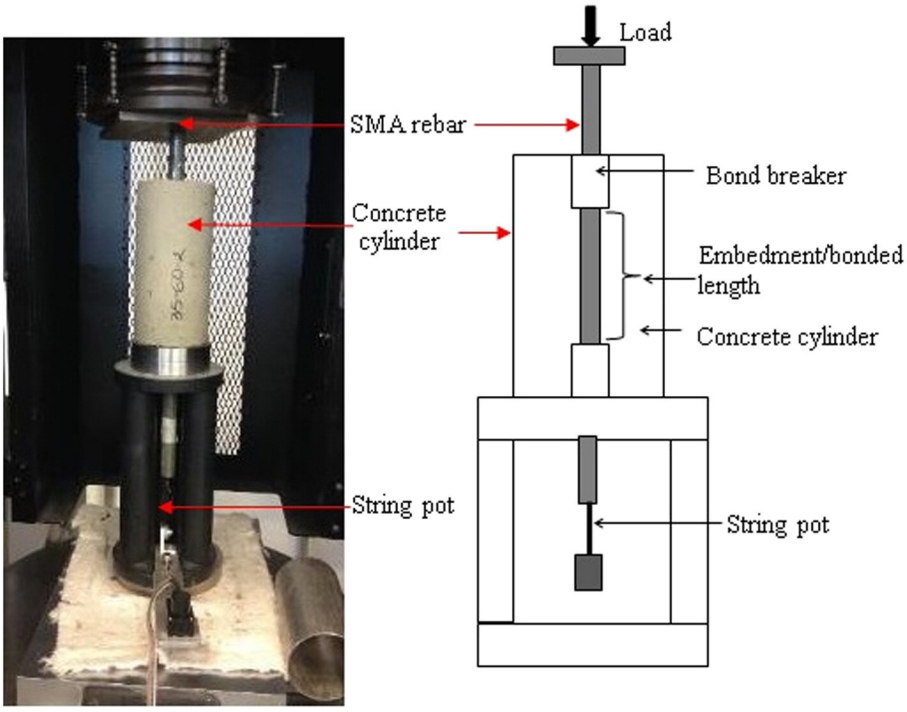

Fig. 4. Test setup for bond behavior SMA rebar with concrete.

On the other hand, for all the sand coated SMA rebars, failure took place at the interface between the SMA bar and the surrounding concrete (Fig. 6). Splitting cracks developed on the concrete bearing surface which extended along the perimeter and continued down the length of the specimens for all the cylinders with 20 mm sand coated SMA rebars. In the case of 32 mm bars coated with 600 μm sand, it showed similar crack pattern while the 32 mm bars coated with 300 μm sand only experienced minor radial cracks developed on the concrete bearing surface. However, the radial cracks did not extend to the specimen perimeter for cylinders with 32 mm SMA rebars coated with 300 μm sand.

4.2. Load–slip relationship and bond strength

After processing the data obtained from the pushout tests, the load–slip relationship for each test was obtained. Typical load–slip behavior of smooth SMA rebar is shown in Fig. 7 for a 100 × 200 mm specimen having a 20 mm diameter bar, 60 mm embedment length, and 40 mm concrete cover. The load–slip curve consists of four parts: (I) elastic stage, (II) ascending branch up to peak load, (III) linearly descending branch, and (IV) residual branch. Fig. 7 also shows the four stages in the load–slip curve. The elastic stage is defined when there is almost no slip with the increase in load and the adhesion bond mechanism plays the major role in transferring the load between SMA and concrete. When the adhesion bond starts to break, the ascending branch starts and continues up to the maximum load, P_{max} at little slip. In the descending stage, the peak load starts to drop suddenly with significant increase in slip value. As slip increases, the wedging action of small particles provide the sole bond mechanism. At the residual stage, the load dropped asymptotically to a limiting residual load P_{res} and the slip values increased quite quickly.

In this study, the bond strength (τ) of an SMA bar embedded in concrete is assumed to be distributed uniformly over the embedment

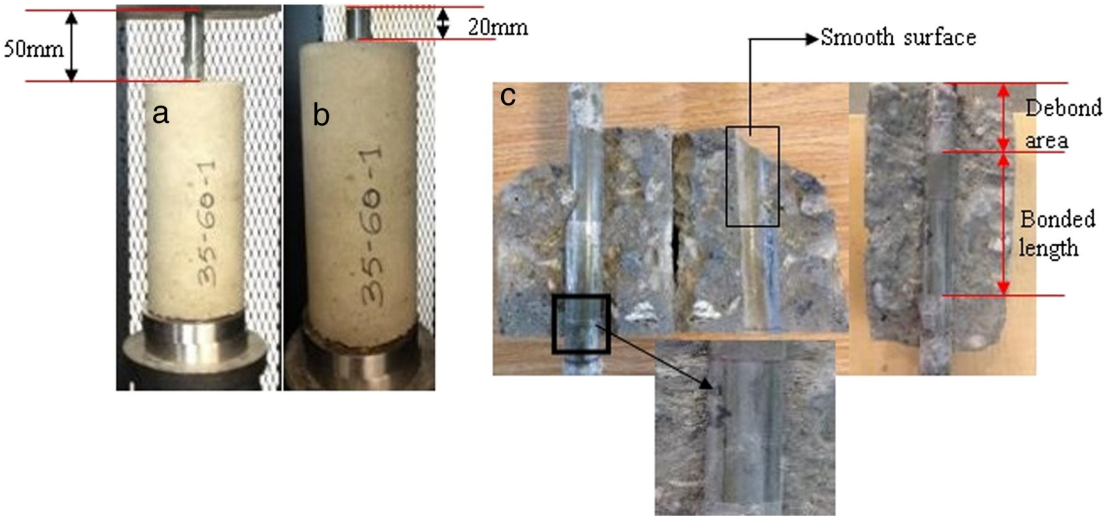

Fig. 5. Specimens (smooth) (a) before testing, (b) after testing and (c) inside view.

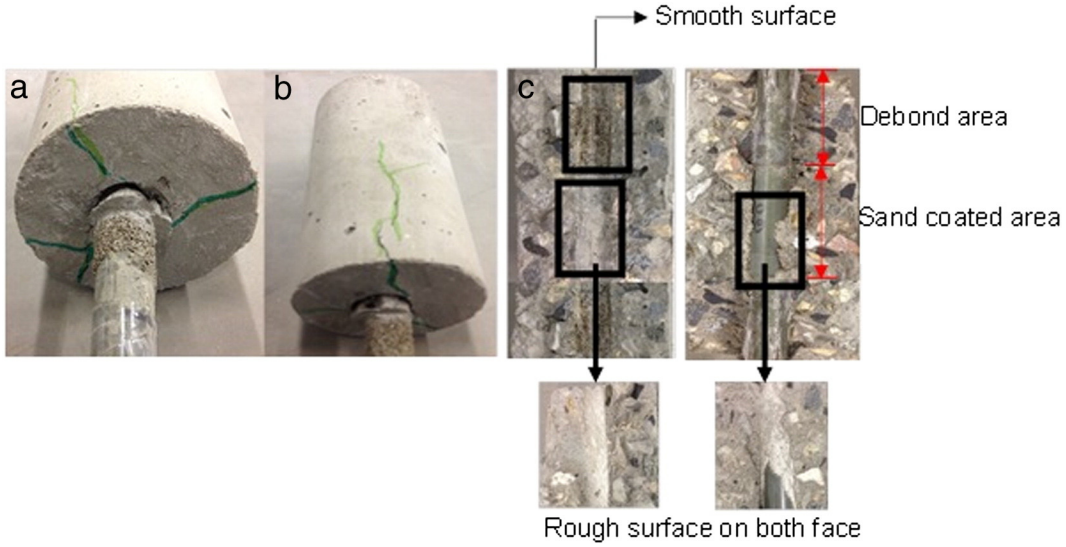

Fig. 6. Failure pattern of sand coated bars' (a) radial cracking, (b) crack propagation in concrete and (c) inside view.

length (L_d). At any stage of loading, the maximum average bond strength can be calculated using Eq. (1):

$$\tau_{\max} = \frac{P_{\max}}{\pi d_b L_d} \tag{1}$$

where, P_{max} is the maximum load obtained from the load slip relation, d_b is the bar diameter, and L_d is the embedment length. In this study, the bond behavior of SMA rebar is investigated in terms of maximum and residual bond strength. The average maximum bond strength (τ_{max}) can be calculated using Eq. (1) and the residual bond strength (τ_{res}) is calculated using Eq. (2):

$$\tau_{res} = \frac{P_{res}}{\pi d_b L_d} \tag{2}$$

where, P_{res} is the residual load obtained from load–slip curve.

4.3. Influencing factor analysis

The impact of different variables considered in this study was investigated individually to find their effect on the bond strength variability. The following sections discuss the effect of various parameters on bond strength of SMA rebar in concrete.

4.3.1. Effect of concrete strength

For investigating the effect of concrete compressive strength, four different concrete strengths were considered. Keeping the embedment length and concrete cover constant at 60 mm and 40 mm, respectively, a total of eight specimens were tested to evaluate the influence of concrete strength on bond behavior of smooth SMA rebar with concrete. Fig. 8 shows the effect of concrete strength on the maximum and the residual bond strength. Separate regression analyses revealed that both maximum and residual bond strength are functions of the square root concrete compressive strength. This is coherent with the findings of other researchers [1,10] on plain rebar and as per the current North American standards [17,18]. From Fig. 7 it can be observed that, both maximum and residual bond strength increase with an increase in concrete compressive strength and this increase is proportional to the square root of the compressive strength. A regression analysis of the test results for which the maximum average bond strength of smooth SMA rebar were measured, yielded the following Eq. (3).

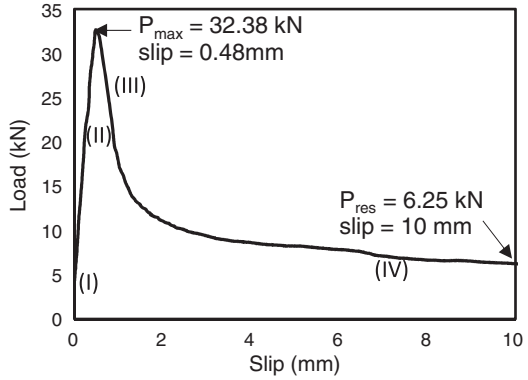

Fig. 7. Load–slip curves for pushout test of smooth SMA rebar.

$$\tau_{\max} = 4.5\sqrt{f_c'} - 22 \tag{3}$$

where, τ_{max} is maximum average bond strength in MPa. This equation can predict the bond strength very well for concrete with compressive strength of up to 40 MPa, but at a higher strength there is a variation of approximately ± 1.5 MPa. However, maximum bond strength of 11.76 MPa was obtained when the concrete strength was 60 MPa which is quite high for plain rebar. However, it should be noted that such large number was obtained for some specimens having an embedment length of $3d_b$ (i.e. not necessarily standard for pushout test specimens). It can be understood from the fact that with the increased embedment length, the probabilities of having imperfect bond between rebar peripheral surface and concrete increases. Hence, for specimens with shorter embedment length is expected to have larger bond strength compared to those of having longer embedment length. This has been explained in detail in Section 4.3.3 which addresses the effect of embedment length.

4.3.2. Effect of bar diameter

Fig. 9 compares the average maximum and residual bond strength of 20 mm and 32 mm smooth SMA rebars. From Fig. 9a it is evident that, as the bar diameter increases the average maximum bond strength decreases. However, no significant influence of bar diameter was observed in the case of average residual bond strength. Since, the results presented in Fig. 9 had different concrete strengths, the bond strength is normalized by the square root of concrete compressive strength. In general, the average maximum bond strength of 20 mm bar was 30%–45% higher than that of 32 mm bar. From the test results, it was observed

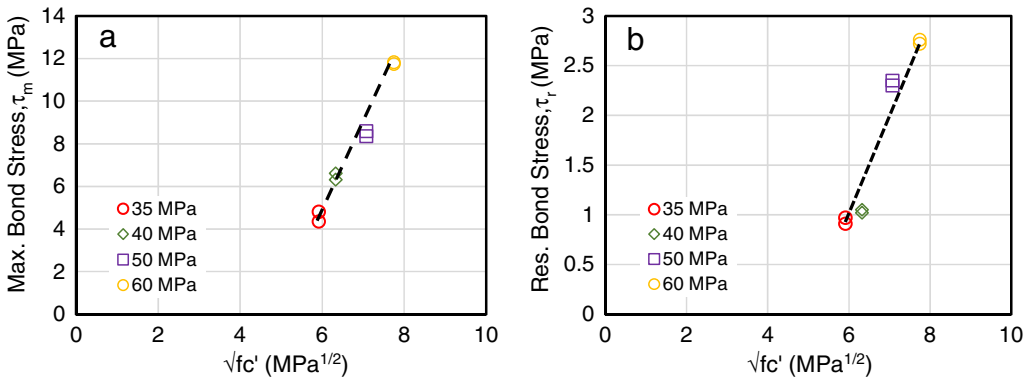

Fig. 8. Effect of concrete compressive strength on average (a) maximum and (b) residual bond strength of smooth SMA bar.

that the effect of bar diameter was more pronounced for concrete with lower strength (35 and 40 MPa) as compared to high strength concrete (50 and 60 MPa). For low strength concrete, the bond strength increased as high as 45% for 20 mm bar as compared to 32 mm bar. In contrast, the bond strength of 32 mm bar decreased by 30% for high strength concrete. This can be attributed to the fact that larger diameter bars require longer embedment length for developing adequate bond strength. Moreover, the Poisson effect with increasing diameter would reduce the adhesion thereby reduces the bond strength.

Using the test results, relationship between bond strength of smooth SMA bar and its bar diameter can be expressed as follows:

$$\tau_{max}/\sqrt{f_c'} = 1.25 - 0.025d_b \quad (4)$$

where, d_b is the bar diameter. Comparison with experimental result showed that Eq. (4) relates very well for smaller diameter as compared to the large diameter. For 20 mm rebar the average absolute error was 3.2% while that for 32 mm rebar was 6.5%.

4.3.3. Effect of embedment length

Four different embedment lengths ($3d_b$, $5d_b$, $7d_b$, $9d_b$) were considered to evaluate their influence on bond strength of smooth SMA rebar. Different embedment lengths for the same diameter were used to assess the effect of embedment length on bond properties of SMA bars. Although pushout tests are usually conducted with standard bond length of $5d_b$, different bond lengths were considered to understand the bond strength and its variability over different embedment length to diameter ratio. Moreover, different embedment length allowed producing a range of bond strengths to get a broader view of the effect of embedment length. Fig. 10 shows the effect of embedment length on the average maximum and residual bond strength of SMA rebar. From Fig. 10 it is evident that the average maximum and residual bond strength increases as the embedment length decreases. Similar behavior has also been reported in literature for steel [12] and FRP rebar [14]. In this study, the increase in average maximum bond strength is more pronounced in small diameter bars as compared to the large diameter ones. For instance, the average maximum bond stress of the $3d_b$ specimens are almost 40% higher as compared to $7d_b$ specimens of 20 mm smooth SMA bars. On the other hand, for the 32 mm bars the same increased by only 27%. This can be attributed to the fact that as the embedment length increases, the surface area over which the SMA bar is bonded to the concrete increases. This increased surface area results in a reduced average bond stress between the bar and the surrounding concrete and also reduces the average stress transferred into the surrounding concrete. A regression analysis of the test results yielded the following quadratic relationship between the normalized bond strength ($\tau_{max}/\sqrt{f_c'}$) of smooth SMA rebar and its embedment length:

$$\tau_{max}/\sqrt{f_c'} = 10^{-5}l_d^2 - 0.005l_d + 1.05. \quad (5)$$

This quadratic relationship is in contrast with the behavior of deformed rebar where there is a liner relation between bond strength

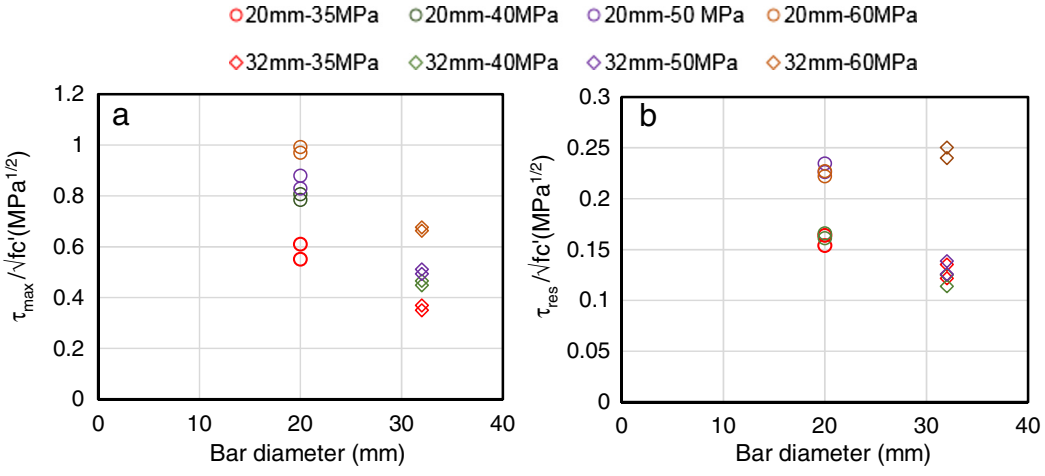

Fig. 9. Effect of bar diameter on average (a) maximum and (b) residual bond strength of smooth SMA bar.

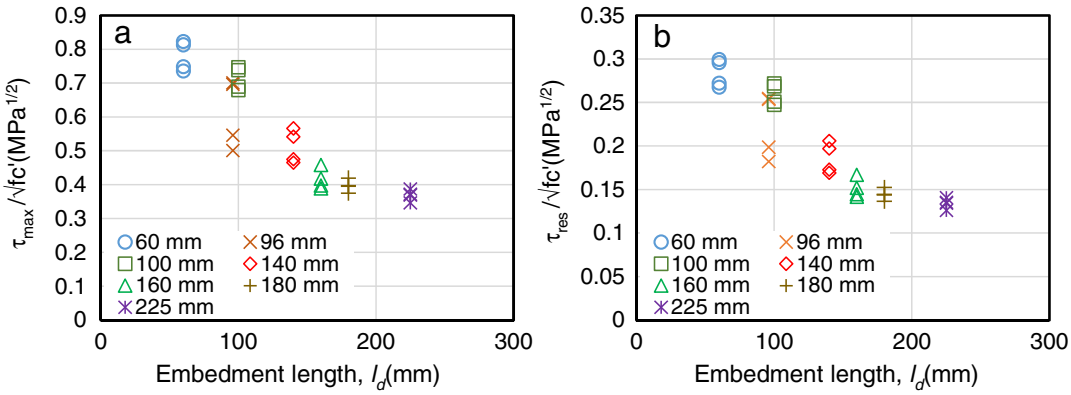

Fig. 10. Effect of embedment length on average (a) maximum and (b) residual bond strength of smooth SMA bar.

and embedment length. In order to verify this finding with the existing design codes and guidelines, a comparison of bond strength obtained from different code recommended equations and results obtained from this study were compared and shown in Table 2. From Table 2, it can be observed that all the code recommended bond strength equation and the result of this study follow the same trend which indicated as the embedment length increases the bond strength decreases. Moreover, a comparison of the bond strength of two different diameter rebar with different embedment length with concrete strength of 35 MPa is provided in Table 3. From this table, it can be observed that for both 20 mm and 32 mm bars, as the embedment length increases from $3d_b$ to $5d_b$ the bond strength decreases by 7.5% and 8.2% respectively, for 20 mm and 32 mm bar. This comparison shows that, irrespective of bar diameter as the embedment length increases the average bond strength decreases by almost the same amount. In a recent study on pushout test of GFRP bars, Hossain et al. [16] found that bond strength of $10d_b$ specimens reduced by 50% as compared to specimens with an embedment length of $3d_b$. Li et al. [9] conducted pushout tests on specimens with embedment lengths ranging from $2.5d_b$ to $8.5d_b$ and concluded that increased embedment length decreases the bond strength.

4.3.4. Effect of concrete cover

The test results were used to determine the effect of concrete cover on the bond behavior of smooth SMA bars. The effect of cover concrete was investigated in terms of cover to bar diameter ratio (c/d_b). Fig. 11 shows the variation in average maximum and residual bond strength of smooth SMA bar with changing cover to bar diameter ratios. From Fig. 11 it is observed that c/d_b has noticeable impact on maximum bond strength, however, residual bond strength was independent of c/d_b. The influence of c/d_b is higher for smaller diameter bars as compared to large diameter ones. From Fig. 11a it can observed that, for 20 mm bars, as the c/d_b increases from 2 to 3.25 (1.625 times) the average maximum bond strength increases by 14%. On the other hand, for 32 mm bars, as the c/d_b increases from 1.06 to 1.84 (1.74 times), the average maximum bond strength increases by 6.5%. A regression analysis of the test results yielded the following quadratic relationship between the normalized bond strength ($\tau_{max}/\sqrt{f_c'}$) of smooth SMA bar and its cover to bar diameter ratio (c/d_b):

$$\tau_{max}/\sqrt{f_c'} = 0.09\left(\frac{c}{d_b}\right)^2 - 0.20\frac{c}{d_b} + 0.82. \quad (6)$$

4.3.5. Effect of surface modification

Previous research on smooth steel and FRP rebars have shown that surface modification of the plain rebars can improve the bond strength significantly [11,21]. However, several researchers have concluded that rebar surface does not appear to affect the bond strength of FRP rebars in concrete [14,22]. The smooth SMA rebars used in this study were modified using two different types of sand in order to improve the bond behavior. Due to the importance of rebar surface on the bond behavior, it is worth investigating the variation in bond behavior with different surface finish. Fig. 12 shows bond strength–slip curves for specimens having different surface finishes with 20 mm bars, l_d of 60 mm and 40 mm cover. Observation from Fig. 12a revealed that, the sand coating significantly improves the bond behavior of smooth rebar. The maximum average bond strength of 600 μm sand coated rebar was 45% and 37% higher than the smooth and 300 μm sand coated rebar, respectively. The maximum average bond strength of 300 μm sand coated bar was 12% higher than that of smooth SMA rebar. However, the maximum average bond strength of 600 μm sand coated

Table 2
Comparison of bond strength calculated from different codes.

Code	Embedment length (mm)		Bond strength (MPa)	
	20 mm	32 mm	20 mm	32 mm
CEB-FIP-2010	480	896	4.17	3.57
ACI-318	580	992	3.45	3.23
IS-2005	620	1056	3.23	3.03
EC-2	440	832	4.55	3.85
AASHTO-2007	560	1408	3.57	2.27
CSA-S6-14	340	563	5.88	5.68
This Study	140	225	2.81	2.29

Concrete strength = 35 MPa, fy = 400 MPa.

Table 3
Variation in bond strength with different embedment length.

Bar diameter	L_d	L_d (mm)	τ_{max} (Mpa)	τ_{avg} (Mpa)
20	$3d_b$	60	4.35	4.38
20	$3d_b$	60	4.41	
20	$5d_b$	100	4.08	4.05
20	$5d_b$	100	4.02	
20	$7d_b$	140	2.81	2.78
20	$7d_b$	140	2.75	
32	$3d_b$	96	4.12	4.13
32	$3d_b$	96	4.14	
32	$5d_b$	160	3.81	3.79
32	$5d_b$	160	3.77	
32	$7d_b$	224	2.49	2.45
32	$7d_b$	224	2.4	

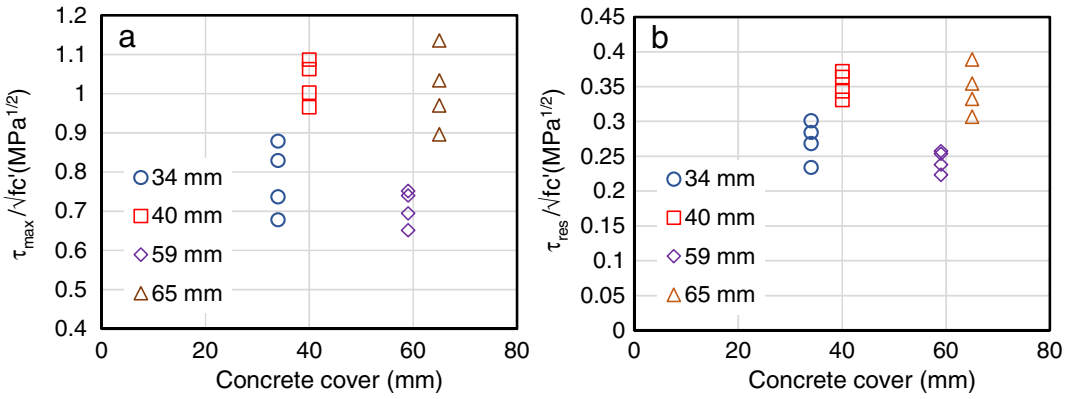

Fig. 11. Effect of concrete cover to bar diameter ratio on average (a) maximum and (b) residual bond strength of smooth SMA bar.

bar was 45% higher than that of smooth SMA rebar. This shows that, the 600 μm sand coating was more effective than the 300 μm sand coating. The average residual bond strength of 600 μm sand coated rebar was 29% and 35% higher than the smooth and 300 μm sand coated rebar, respectively. Interestingly, average residual bond strength of 300 μm sand coated rebar was 6% lower than that of smooth rebar.

Panels b and c in Fig. 12 show the influence of rebar diameter and embedment length on the bond strength behavior of SMA rebars with different surface finishes. Similar trend was observed for all the bars irrespective of bar finish; the bond strength decreases as the bar diameter and embedment length increases. From Fig. 12b it can be observed that, the 32 mm sand coated bars produced higher maximum average bond strength as compared to smooth 32 mm bars. Similar conclusion can be drawn on the effect of embedment length. Fig. 12c shows that the 600 μm sand coated bars with different embedment lengths produces higher bond strength as compared to those of smooth rebars and 300 μm sand coated bars. It can be concluded that the friction and interlocking produced by the roughened surface creates a more effective mechanism and improves the bond of smooth SMA rebar significantly.

5. Empirical relationship for bond strength of SMA rebar

The analysis results presented and discussed on previous sections revealed the influence of different factors and surface condition on the bond strength of SMA rebar with concrete. Regression analysis of all the specimens, considering all influential parameters, yields the following equation:

$$\tau_{max} = k_r\left(0.9 - 0.004d_b - 0.0025l_d + 0.015\frac{c}{d_b}\right)\sqrt{f_c'} \quad (7)$$

where, τ_{max} is the average maximum bond strength in MPa, d_b is the bar diameter in mm, l_d is the embedment length in mm, c is the concrete

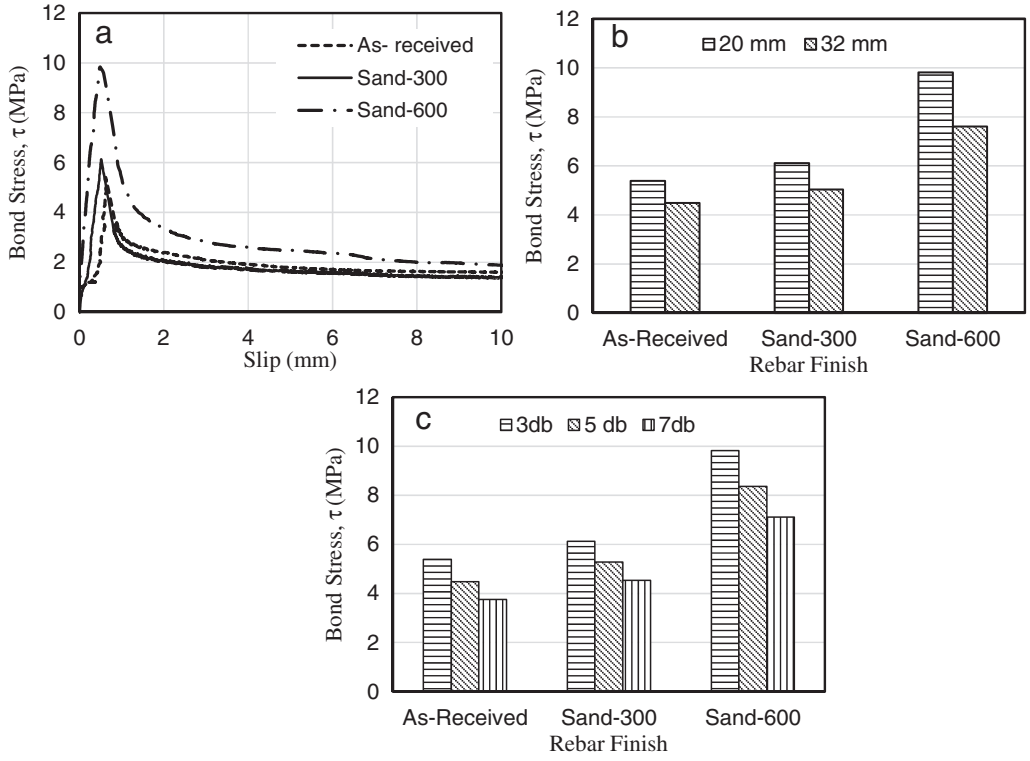

Fig. 12. Effect of sand coating on bond strength of SMA rebar (a) bond stress–slip curve, (b) effect of bar diameter and (c) effect of embedment length.

cover in mm, f_c' is the concrete compressive strength in MPa, and k_r is the surface roughness factor which is 1 for smooth rebar. In the case of sand coated rebar, k_r can be calculated using Eq. (8).

$$k_r = 0.17\alpha^2 - 1.92\alpha + 6.5 \tag{8}$$

where, α is the sand size coefficient and calculated as, $\alpha = 2/\text{sand size in mm}$.

The proposed Eq. (7) can be used to estimate the bond strength of SMA rebar in concrete considering both smooth and sand coated surface. To verify the accuracy of the proposed equation, comparison was made with experimental results. Fig. 13 shows the comparison of normalized bond strength obtained from the test results and the proposed equation. Fig. 13 shows that the proposed equation predicted the bond strength very well where the correlation coefficient is 0.916.

6. Comparison with bond behavior of sand coated FRP bars

For comparative analysis, the bond strength of sand coated FRP bars provided by different design codes are compared with sand coated SMA rebars tested in this study. The average bond strength determined from experimental results and using Eq. (7) are compared with the bond strength calculated as per CSA S806-12 [23] and CSA S6-10 [24]. ACI 440.1R-06 [25] was not considered since the ACI equation warrants the development length to be at least $19d_b$ and the equation was developed based on concrete strength between 28 MPa and 45 MPa. Since in this study, the sand coated SMA rebars were tested with 50 MPa concrete and embedment length of $3d_b$–$7d_b$, the ACI equation may not be accurate to predict the bond strength of sand coated SMA rebar.

Canadian Standards Association CSA S806-12 [23]) provides the following equation (Eq. (9)) for calculating the development length of FRP Bars.

$$l_d = \frac{1.5k_1k_2k_3k_4k_5}{d_{cs}}\frac{f_F}{\sqrt{f_c'}}A_b \tag{9}$$

Using Eq. (9), the following equation was derived to calculate the bond strength of FRP rebar:

$$\tau_{\max} = \frac{d_{cs}\sqrt{f_c'}}{1.5k_1k_2k_3k_4k_5\pi d_b} \tag{10}$$

where, d_{cs} = smallest of the distance from the closest concrete surface to the center of the bar being developed or two-thirds the center to center spacing of the bars being developed (mm), f_c' = compressive strength of concrete (MPa); k_1 = bar location factor (1.3 for horizontal reinforcement placed so that more than 300 mm of fresh concrete is cast below the bar; 1.0 for all other cases); k_2 = concrete density factor (1.3 for structural low-density concrete; 1.2 for structural semi-low-density concrete; 1.0 for normal density concrete); k_3 = bar size factor (0.8 for $A_b < 300$ mm^2; 1.0 for $A_b > 300$ mm^2); A_b is the cross-sectional area of an individual bar in mm^2; k_4 = bar fiber factor (1.0 for CFRP and GFRP; 1.25 for AFRP); k_5 = bar surface profile factor (1.0 for surface roughened or sand coated or braided surfaces; 1.05 for spiral pattern surfaces or ribbed surfaces; 1.8 for indented surfaces).

According to the Canadian Highway Bridge Design Code [24], the expression for the bond strength of FRP rebar is calculated as follows:

$$\tau_{\max} = \frac{\left(d_{cs} + k_{tr}\frac{E_{frp}}{E_s}\right)}{0.45k_1k_6\pi d_b}f_{cr}; \tag{10}$$

$$k_{tr} = \frac{A_{tr}f_y}{10.5sn}; \left(d_{cs} + k_{tr}\frac{E_{frp}}{E_s}\right) \le 2.5d_b \tag{11}$$

where, A_{tr} = area of transverse reinforcement normal to the plane of splitting through the bars (mm^2); f_y = yield strength of transverse reinforcement (MPa); s = center to center spacing of the transverse reinforcement (mm); n = number of bars being developed along the plane of splitting; E_{FRP} = modulus of elasticity of FRP bar (MPa); E_s = modulus of elasticity of steel (MPa); k_6 is bar surface factor, f_{cr} is the flexural strength of concrete in MPa ($0.4\sqrt{f_c'}$ for normal density concrete, $0.34\sqrt{f_c'}$ for semi-low density concrete, $0.30\sqrt{f_c'}$ for low-density concrete).

Table 4 shows the comparison of sand coated SMA rebars obtained from pushout tests and prediction equation with those obtained from the two design codes. Table 4 shows that the embedment length and concrete cover have no influence on the bond strength according to CSA-S806-12 [23] and CSA S6-10 [24]. Since no transverse reinforcement were provided in pushout specimens, the confinement effect provided by lateral reinforcement index, k_{tr}, in CSA S6-10 [24] can be neglected. From Table 4 it can be observed that the bond strength obtained using CSA S6-10 [24] have a closer match with the experimental and predicted bond strength of sand coated SMA bars. On the contrary, the bond strength calculated using CSA-S806-12 [23] varies by a large margin. From the results presented in Table 4, it can be concluded that with few modifications, the CSA S6-10 [24] equation for bond strength prediction of sand coated FRP rebar can be used for the bond strength prediction of sand coated SMA rebar. However, the proposed bond strength equation is not suggested to be used for sand coated FRP rebar since design of FRP reinforced concrete members would require certain other considerations.

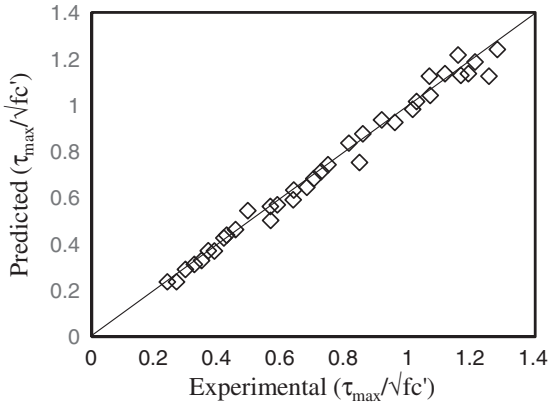

Fig. 13. Comparison between experimental and predicted values of $\tau_{max}/\sqrt{f_c'}$.

Table 4
Comparison of bond strength sand coated SMA bars with sand coated FRP bars.

Rebar type	Experiment MPa	Prediction MPa	CSA S6-10 MPa	CSA S806-12 MPa
20-300-3d_b	6.12	6.24	6.25	4.89
20-300-5d_b	5.28	5.35	6.25	4.89
20-300-7d_b	4.54	4.45	6.25	4.89
20-600-3d_b	9.82	9.80	6.25	4.89
20-600-5d_b	8.36	8.40	6.25	4.89
20-600-7d_b	7.11	7.00	6.25	4.89
32-300-3d_b	5.04	4.88	3.91	3.06
32-300-5d_b	3.37	3.46	3.91	3.06
32-600-3d_b	7.61	7.67	3.91	3.06
32-600-5d_b	5.48	5.43	3.91	3.06

Sample designation: bar dia-sand size-embedment length.
Concrete cover = 40 mm and concrete strength = 50 MPa.

7. Summary and conclusions

This study investigated the bond behavior of smooth and sand coated shape memory alloy bars in concrete. Experimental investigations were carried out using pushout tests to investigate the influence of concrete strength, bar diameter, concrete cover, embedment length, and surface condition on the bond strength of SMA rebar. The results from 56 pushout tests lead to the following conclusions:

1. The stress–slip curve of SMA rebar can be divided/idealized into four stages: elastic stage, ascending stage, linearly descending stage and residual stage.
2. The surface roughness of SMA rebar significantly affects the failure pattern as well as the bond strength. Concrete with smooth SMA rebars resulted in simple pushout failure whereas sand coated rebars resulted in splitting failure.
3. The bond strength of both smooth and sand coated SMA rebar is significantly influenced by the concrete strength, bar diameter and embedment length but is independent of concrete cover.
4. The application of sand coating increased the bond strength between concrete and SMA rebar by developing friction and interlocking forces in addition to the adhesion mechanism. The coarser the sand size, the more is the improvement in bond strength.
5. A new equation for calculating the bond strength of SMA rebar in concrete is proposed based on the experimental study. For different strengths of concrete, bar diameters, surface condition and embedment length, the proposed equation is in good agreement with the experimental results.

The present study only considered pushout tests for investigating the bond behavior of SMA rebar in concrete. Further study need to be conducted considering SMA reinforced beams with and without lateral reinforcement. Further study needs to be carried out considering different types of SMA rebar to develop a more comprehensive bond–slip relationship for SMA rebar in concrete.

Acknowledgment

The authors gratefully acknowledge the assistance of the following: Ryan Mandu, UBC Structures Laboratory Technician, for assistance with the test setup; Dr. Nouroz Islam, for assistance with the data acquisition system setup; Kader, Sumaiya, and Anant, graduate students at UBC, for assistance in concrete casting. The financial contributions of the Natural Sciences and Engineering Research Council of Canada (NSERC) through the Discovery Grant (2014-2019) and Industrial Postgraduate Scholarship Program were critical in conducting this study and are gratefully acknowledged.

References

[1] Wu Z, Zhang X, Zheng J, Hu Y, Li Q. Bond behavior of plain round bars embedded in concrete subjected to biaxial lateral tensile-compressive stresses. ASCE J Struct Eng 2014;140(4):1–11.
[2] ACI Committee 408. Bond and development of straight reinforcing bars in tension (ACI 408R-03). American Concrete InstituteFarmington Hills, Mich.; 2003
[3] Youssef MA, Alam MS, Nehdi M. Experimental investigation on the seismic behavior of beam-column joints reinforced with superelastic shape memory alloys. J Earthquake Eng 2008;12(7):1205–22.
[4] Saiidi MS, O'Brien M, Zadeh MS. Cyclic response of concrete bridge columns using superelastic nitinol and bendable concrete. ACI Struct J 2009;106(1):69–77.
[5] Billah AHMM, Alam MS. Seismic performance of concrete columns reinforced with hybrid shape memory alloy (SMA) and fiber reinforced polymer (FRP) bars. Construct Build Mater 2012;28(1):730–42.
[6] Billah AHMM, Alam MS. Seismic fragility assessment of concrete bridge piers reinforced with superelastic shape memory alloy. In press Earthq Spectra 2015; 31(3):1515–41.
[7] Alam MS, Youssef MA, Nehdi M. Utilizing shape memory alloys to enhance the performance and safety of the civil infrastructure: a review. Can J Civil Eng 2007; 34:1075–86.
[8] Li HT, Deeks AJ, Su XZ. Compressive bond slip model of reinforcing bars. J Cent South Univ 2011;42(11):1–7 [in Chinese].
[9] Li H, Deeks A, Su X. Experimental study on compressive bond anchorage properties of 500 MPa steel bars in concrete. J Struct Eng 2013;139(12).
[10] Feldman LR, Bartlett FM. Bond strength variability in pullout specimens with plain reinforcement. ACI Struct J 2005;102(6):860–7.
[11] Mao DL, Liu LX, Fan L. Bond-anchorage properties and proposed design of HRB500 steel bars in concrete. J Zhengzhou Univ 2004;25(2):54–8.
[12] Feldman LR, Bartlett FM. Bond stresses along plain steel reinforcing bars in pullout specimens. ACI Struct J 2007;104(6):685–92.
[13] Verderame GM, Ricci P, Carlo GD, Manfredi G. Cyclic bond behaviour of plain bars. Part I: experimental investigation. Construct Build Mater 2009;23(12):3499–511.
[14] Wambeke BW, Shield CK. Development length of glass fibre-reinforced polymer bars in concrete. ACI Struct J 2006;103(1):11–7.
[15] Hossain KMA, Lachemi M. Bond behaviour of self-consolidating concrete with mineral and chemical admixtures. ASCE J Mater Civil Eng 2008;20(9):608–16.
[16] Hossain KMA, Ametrano D, Lachemi M. Bond strength of standard and high-modulus GFRP bars in high-strength concrete. ASCE J Mater Civil Eng 2014;26(3):449–56.
[17] Canadian Standards Association. CSA standard A23.3–14, design of concrete structures. Ontario, Canada: Rexdale; 2014(295 pp).
[18] ACI Committee 318. Building code requirements for structural concrete (ACI 308-11). American Concrete InstituteFarmington Hills, Mich.; 2011 (503 pp).
[19] Bamonte PF, Gambarova PG. High-bond bars in NSC and HPC: study on size effect and on the local bond stress–slip law. ASCE J Struct Eng 2007;133(2):225–34.
[20] Hao Q, Wang Y, He Z, Ou J. Bond strength of glass fibre reinforced polymer ribbed rebars in normal strength concrete. Construct Build Mater 2009;23(2):865–71.
[21] Arias JPM, Vazquez A, Escobar M. Use of sand coating to improve bonding between GFRP bars and concrete. J Compos Mater 2012;46(18):2271–8.
[22] Mosley CP, Tureyen AK, Frosch RJ. Bond strength of nonmetallic reinforcing bars. ACI Structural Journal 2008;105(5):634–42.
[23] Canadian Standards Association. CAN/CSA-S806-12 — design and construction of building components with fibre reinforced polymers. Canadian Standards AssociationOntario, Canada: Rexdale; 2012.
[24] Canadian Standards Association. CAN/CSA-S6-10—Canadian highway bridge design code. Canadian Standards AssociationOntario, Canada: Rexdale; 2010 (752 pp.).
[25] ACI Committee 440. Guide for the design and construction of structural concrete reinforced with FRP bars (ACI 440.1R-06). American Concrete InstituteFarmington Hills, Mich.; 2006.